International Conference on Mathematics, Computational Methods & Reactor Physics (M&C 2009)
Saratoga Springs, New York, May 3-7, 2009, on CD-ROM, American Nuclear Society, LaGrange Park, IL (2009)

A NON-LINEAR OPTIMAL DISCONTINUOUS PETROV-GALERKIN METHOD FOR STABILISING THE SOLUTION OF THE TRANSPORT EQUATION

S. R. Merton and R. P. Smedley-Stevenson
Computational Physics Group
AWE Aldermaston, Reading, Berkshire RG7 4PR, United Kingdom
simon.merton@awe.co.uk

C. C. Pain, A. G. Buchan and M. D. Eaton
Department of Earth Science and Engineering
Imperial College London, London SW7 2AZ United Kingdom
c.pain@imperial.ac.uk

ABSTRACT

This paper describes a new Non-Linear Discontinuous Petrov-Galerkin (NDPG) method and application to the one-speed Boltzmann Transport Equation (BTE) for space-time problems. The purpose of the method is to remove unwanted oscillations in the transport solution which occur in the vicinity of sharp flux gradients, while improving computational efficiency and numerical accuracy. This is achieved by applying artificial dissipation in the solution gradient direction, internal to an element using a novel finite element (FE) Riemann approach. The amount of dissipation added acts internal to each element. This is done using a gradient-informed scaling of the advection velocities in the stabilisation term. This makes the method in its most general form non-linear. The method is designed to be independent of angular expansion framework. This is demonstrated for the both discrete ordinates (S_N) and spherical harmonics (P_N) descriptions of the angular variable. Results show the scheme performs consistently well in demanding time dependent and multi-dimensional radiation transport problems.

Key Words: SUPG, Radiation Transport, Discontinuous Galerkin, Disctrete Ordinates, Spherical Harmonics

1. INTRODUCTION

The Discontinuous Galerkin (DG) method has received a great deal of attention in modern transport applications. First proposed for computational neutron transport in 1973 by Reed and Hill [1], the DG method has become extremely popular for spatial, temporal, and space-time discretisations of the Boltzmann Transport Equation (BTE). Continuity of solution is not enforced, allowing the capture of sharp flux gradients such as those occurring in the vicinity of dissimilar materials. Although adequate for a broad range of applications, the DG method does however, suffer defects. In certain cases, the discontinuities can result in unwanted oscillations being introduced in the transport solution. This has motivated the use of stabilisation strategies such as Petrov-Galerkin (PG) and Streamline Upwind Petrov-Galerkin (SUPG) methods in radiation transport applications [5, 6]. First introduced by Brooks and Hughes in 1982 for improved shock handling in high speed flows [2, 13–16], these methods improve the smoothness and capture of discontinuities by adding onto the discretisation an upwind term for numerical stability, typically in the streamline direction.

One notable deficiency of the conventional linear upwind approach is that the same amount of artificial dissipation is introduced everywhere throughout the domain, although various approaches have been suggested that optimise it in some sense [4, 7]. These so-called ”optimal” methods are also deficient in that they are based on one length scale chosen to represent the entire domain. For example, the time step may provide a suitable length scale at early times while there is transient behaviour, but becomes unsuitable as steady-state is reached, at which point the element width would be a better choice. However, the element width would not be appropriate at early time where temporal modes dominate the solution field. This can be addressed by introducing non-linearity, using the gradient of the solution to determine a dissipation that is most appropriate locally. Additionally, there are problems where unwanted oscillations occur in the gradient directions. In such cases, applying artificial dissipation only along the streamline direction may not stabilise the solution. It should be applied in the gradient direction, requiring knowledge of the solution thereby making the scheme non-linear. Methods have been developed that scale the magnitude of the dissipation so it is made optimal in the direction of the gradient, using the cosine of the angle between the streamline and gradient vectors[9]. A potential limitation of this approach arises when the gradient is perpendicular to the streamline, as this results in the dissipation being scaled out completely. The non-linear discontinuous Galerkin (NDPG) method proposed in the current paper uses gradient-informed advection velocities in the stabilisation term such that all dissipation acts in the gradient direction only. Artificial dissipation in this direction is then added internal to an element via a novel finite element Riemann approach. Using a Riemann approach makes the new method independent of angular discretisation scheme. The NDPG method can of course be combined with a conventional linear SUPG formulation to stabilise the solution across all radiation regimes.
The paper has been arranged as follows. In section 2 the time dependent linear form of the one-speed Boltzmann Transport Equation (BTE) is introduced and discretised using linear discontinuous finite elements, on both the spatial and temporal grids. No assumption is made regarding the angular scheme; a key feature of this work is that it is independent of the choice of basis function describing direction of particle travel. Consequently, the methods described in this paper operate for arbitrary discretisation in angle. Galerkin weighting is used for both the spatial and temporal projections. A space-time Riemann approach to implementing the boundary conditions is introduced in section 3. This decouples the flow across the element boundaries into a set of independent one dimensional waves, making the scheme independent of the angular discretisation used. In section 4 a linear method is discussed. This uses a fixed length scale, a property that is not entirely satisfactory as it results in the same type of dissipation being applied everywhere throughout the domain. Section 5 introduces non-linearity allowing the type of dissipation to be defined differently at each node according to local behaviour of the solution. Numerical results are presented and discussed in section 6. The non-linear scheme is demonstrated on a series of demanding radiation transport test problem that include time dependent and steady-state cases. This is done for discrete ordinates and spherical harmonics on the sphere. Conclusions are drawn in section 7.

2. SPACE-TIME DISCRETISATION OF THE BOLTZMANN EQUATION

Numerical solutions to the time dependent form of the Boltzmann equation are of great importance in a variety of neutron transport and radiation-hydrodynamics computational problems. Applications range from representing the transient behaviour of reactors and the time

dependent simulation of delayed neutron physics to the modelling of fissile solutions. Temporal discretisation technologies have become as sophisticated as schemes once only considered for spatial domains. The DG method, in particular, is becoming an increasingly popular choice for space-time differencing of the BTE [3]. This allows capture of radiation fields that are exremely poorly behaved. The work in the current paper uses the linear discontinuous Galerkin method on both the spatial and temporal grids, treating time as just another dimension over which the transport takes place. In the case of two spatial dimensions, the resulting element has the same number of unknowns representing the space-time variation as there are in a three-dimensional element of the same polyhedral type and order. This allows the solution to be discontinuous on both the spatial and temporal boundaries of the element. The time dependent, linear form of the one-speed BTE may be written as

$$(\frac{1}{v_g}\frac{\partial}{\partial t} + \mathbf{\Omega}\cdot\nabla + \sigma_t(\mathbf{r},\mathbf{\Omega}))\psi(\mathbf{r},\mathbf{\Omega}) = \mathbf{q}(\mathbf{r},\mathbf{\Omega}) \tag{1}$$

where v_g refers to the group velocity of the neutrons, $\psi(\mathbf{r},\mathbf{\Omega})$ is the angular flux at position $\mathbf{r}$ travelling along direction $\mathbf{\Omega}$ in the continuum, to which computational solutions are required. $\sigma_t(\mathbf{r},\mathbf{\Omega})$ is the scattering-removal cross-section. This describes losses to the host media, and scattering of the particles in angle of transport. It is common practice in radiation transport literature to make the assumption that the scattering-removal cross-section is time independent. In general this will not be the case, and material properties can vary significantly with time for example if effects such as burn-up are included in the simulation. This requires the scattering-removal cross-section to vary in space-time. In the present work, it is assumed that $\sigma_t(\mathbf{r},\mathbf{\Omega})$ is constant with respect to time. $\mathbf{q}(\mathbf{r},\mathbf{\Omega})$ is the sum of all sources driving the system which may include fission, out of group scattering and imposed body sources. In general, these vary in time also. In the current work, scattering is assumed to be isotropic. The inclusion of anisotropy on the scattering term is a straightforward extension to the present work. One may write $\sigma_t(\mathbf{r},\mathbf{\Omega}) = \sigma_a(\mathbf{r}) + \sigma_s(\mathbf{r},\mathbf{\Omega}\rightarrow\mathbf{\Omega}^{'})$ where $\sigma_a(\mathbf{r})$ defines the absorption cross-section and $\sigma_s(\mathbf{r},\mathbf{\Omega}\rightarrow\mathbf{\Omega}^{'})$ the cross-section of a particle initially travelling in direction $\mathbf{\Omega}$ scattered into direction $\mathbf{\Omega}^{'}$. The angular flux emission due to such scattering events results in an extra source term. The scattering kernel $\sigma_s(\mathbf{r},\mathbf{\Omega}\rightarrow\mathbf{\Omega}^{'})$ is then expanded in Legendre polynomials to represent the angular distribution independently of the approximation used to represent the angular flux itself. The direction $\mathbf{\Omega}$ is a vector that defines a point on the surface of the unit sphere, and maybe expressed in terms of Cartesian components $(\Omega_x,\Omega_y,\Omega_z)^T$. This represents all directions of particle travel inside the unit sphere. In order to solve Eq. 1 on a computational mesh to obtain numerical approximations to $\psi(\mathbf{r},\mathbf{\Omega})$, the angular flux must be discretised in space, time and angle. It is usual to perform the angular discretisation first, followed by the spatial and temporal differencing. This results in a symmetric system of coupled hyperbolic equations. One first obtains the angular discrete form of the equation by selecting an appropriate set of basis functions in direction of particle travel. The angular discrete form may be written

$$(\mathbf{A}\cdot\nabla + \mathbf{H}(\mathbf{r}))\mathbf{\Psi}(\mathbf{r}) - \mathbf{S}(\mathbf{r}) = \mathbf{0} \tag{2}$$

in which $\mathbf{A}$ is a vector of space-time invariant angular Jacobian matrices $(\mathbf{A}_t,\mathbf{A}_x,\mathbf{A}_y,\mathbf{A}_z)^T$, and $\mathbf{H}(\mathbf{r})$ the angular discretised scattering removal matrix operator at position $\mathbf{r}$ in space-time. $\mathbf{\Psi}(\mathbf{r})$

is the angular discrete flux at position $\mathbf{r}$ in space-time. This comprises a vector of $\mathcal{M}$ unknowns at position $\mathbf{r}$ in space-time, i.e. $\mathbf{\Psi}(\mathbf{r}) = (\mathbf{\Psi_1}(\mathbf{r}), ..., \mathbf{\Psi}_{\mathcal{M}}(\mathbf{r}))^{\mathbf{T}}$. Therefore $\mathbf{H}(\mathbf{r})$ is a rank-2 matrix of dimension $\mathcal{M}$. $\mathbf{S}(\mathbf{r})$ is the angular discrete source vector at position $\mathbf{r}$ in the space-time domain, i.e. $\mathbf{S}(\mathbf{r}) = (\mathbf{s_1}(\mathbf{r}), ..., \mathbf{s}_{\mathcal{M}}(\mathbf{r}))^{\mathbf{T}}$. Note that Eq. 2 is independent of angular scheme. One may use discrete ordinate (S_N), spherical harmonic (P_N) or wavelet (LW_N) methods without having to alter Eq. 2. Consequently, the work that follows is completely general and not specific to any particular deterministic method. Once the angular part is complete, one is in a position to perform the spatial and temporal discretisation. A suitable set of nodal basis functions $\mathbf{N}(\mathbf{r})$ are chosen, where $\mathbf{N}_i(\mathbf{r})$ is a diagonal $\mathcal{M} \times \mathcal{M}$ matrix with the node i basis function along the main diagonal. Eq. 2 is multiplied through by $\mathbf{N}_i(\mathbf{r})$ and integrated by parts over the element domain V_e (the boundary of V_e is Γ_e). Integration by parts produces a surface integral that couples the elements across the spatial and temporal meshes. One then substitutes $\Psi(\mathbf{r}) = \sum_j \mathbf{N}_j(\mathbf{r})\phi_j$ and $\mathbf{S}(\mathbf{r}) = \sum_{\mathbf{j}} \mathbf{N_j}(\mathbf{r})\mathbf{s_j}$ to obtain the discrete system of equations

$$\int_{V_e} (-\mathbf{A}\cdot\nabla\mathbf{N}_i(\mathbf{r})\sum_j \mathbf{N}_j(\mathbf{r})\Psi_j + \mathbf{N}_i(\mathbf{r})\mathbf{H}\sum_j \mathbf{N}_j(\mathbf{r})\Psi_j - \mathbf{N}_i(\mathbf{r})\sum_j \mathbf{N}_j(\mathbf{r})s_j)dV + \int_{\Gamma_{ein}} \mathbf{n}\cdot\mathbf{A}\mathbf{N}_i(\mathbf{r})\Psi_{IN}d\Gamma + \int_{\Gamma_{eout}} \mathbf{n}\cdot\mathbf{A}\mathbf{N}_i(\mathbf{r})\Psi d\Gamma = \mathbf{0} \tag{3}$$

Thus each node pair i, j has a matrix block of size $\mathcal{M} \times \mathcal{M}$ associated with it, $\mathcal{M}$ being the number of unknowns on the sphere. The solution at node i is a vector of length $\mathcal{M}$ containing the moments of the flux at that point in space-time. Ψ_{IN} is the boundary condition coming in from either a neighbouring element or the edge of the domain, and $\mathbf{0}$ a vector of length $\mathcal{M}$ containing zeroes. Note that when integration by parts is applied to the advection terms, the troublesome derivatives on the element boundaries are removed in addition to creating the surface integral that contains the boundary conditions. In Eq. 4 this surface term has been split into an inbound contribution $\Gamma_{e_{IN}}$ and an outbound contribution $\Gamma_{e_{OUT}}$. This approach fully upwinds the solution on the incoming boundaries of the element on the spatial and temporal grids of the solution domain.

3. SPACE-TIME BOUNDARY CONDITIONS

Space-time boundary conditions are implemented via a finite element Riemann approach. This involves examining the eigenstructure of the Jacobian matrices $\mathbf{A}_x, \mathbf{A}_y, \mathbf{A}_z$ and $\mathbf{A}_t$ in order to decouple outbound information from inbound information. These eigenstructures are obtained by taking the Riemann decompostion of each angular Jacobian, giving the matrices of left and right eigenvectors and the diagonal matrix of eigenvalues, for each. That is to use

$$\mathbf{A}_x = \mathbf{L}_x\mathbf{\Lambda}_x\mathbf{R}_x, \quad \mathbf{A}_y = \mathbf{L}_y\mathbf{\Lambda}_y\mathbf{R}_y, \quad \mathbf{A}_z = \mathbf{L}_z\mathbf{\Lambda}_z\mathbf{R}_z, \quad \mathbf{A}_t = \mathbf{L}_t\mathbf{\Lambda}_t\mathbf{R}_t \tag{4}$$

where $\mathbf{L}_x, \mathbf{L}_y, \mathbf{L}_z, \mathbf{L}_t$ are the matrices of left eigenvectors, $\mathbf{R}_x, \mathbf{R}_y, \mathbf{R}_z, \mathbf{R}_t$ the matrices of right eigenvectors and $\mathbf{\Lambda}_x, \mathbf{\Lambda}_y, \mathbf{\Lambda}_z, \mathbf{\Lambda}_t$ the diagonal matrices of eigenvalues associated with the

Riemann decompostion of $\mathbf{A}_x, \mathbf{A}_y, \mathbf{A}_z, \mathbf{A}_t$ respectively. Positive eigenvalues correspond with outbound information on the element boundaries and negative eigenvalues correspond with incoming information. Once the eigenstructures are obtained, the components of each eigenvalue matrix $\mathbf{\Lambda}_x, \mathbf{\Lambda}_y, \mathbf{\Lambda}_z, \mathbf{\Lambda}_t$ are sorted by sign in the Riemann space where they are diagonal. This involves constructing two diagonal sorting matrices for each axis to decouple the directions into separate inbound and outbound modes

$$\mathbf{\Lambda}^+_{x_{ii}} = \begin{cases} \mathbf{\Lambda}_{x_{ii}} & \mathbf{\Lambda}_{x_{ii}} \cdot n_x \geq 0; \\ 0 & \mathbf{\Lambda}_{x_{ii}} \cdot n_x < 0. \end{cases} \quad , \quad \mathbf{\Lambda}^-_{x_{ii}} = \begin{cases} \mathbf{\Lambda}_{x_{ii}} & \mathbf{\Lambda}_{x_{ii}} \cdot n_x < 0; \\ 0 & \mathbf{\Lambda}_{x_{ii}} \cdot n_x \geq 0. \end{cases}$$

$$\mathbf{\Lambda}^+_{y_{ii}} = \begin{cases} \mathbf{\Lambda}_{y_{ii}} & \mathbf{\Lambda}_{y_{ii}} \cdot n_y \geq 0; \\ 0 & \mathbf{\Lambda}_{y_{ii}} \cdot n_y < 0. \end{cases} \quad , \quad \mathbf{\Lambda}^-_{y_{ii}} = \begin{cases} \mathbf{\Lambda}_{y_{ii}} & \mathbf{\Lambda}_{y_{ii}} \cdot n_y < 0; \\ 0 & \mathbf{\Lambda}_{y_{ii}} \cdot n_y \geq 0. \end{cases}$$

$$\mathbf{\Lambda}^+_{z_{ii}} = \begin{cases} \mathbf{\Lambda}_{z_{ii}} & \mathbf{\Lambda}_{z_{ii}} \cdot n_z \geq 0; \\ 0 & \mathbf{\Lambda}_{z_{ii}} \cdot n_z < 0. \end{cases} \quad , \quad \mathbf{\Lambda}^-_{z_{ii}} = \begin{cases} \mathbf{\Lambda}_{z_{ii}} & \mathbf{\Lambda}_{z_{ii}} \cdot n_z < 0; \\ 0 & \mathbf{\Lambda}_{z_{ii}} \cdot n_z \geq 0. \end{cases}$$

$$\mathbf{\Lambda}^+_{t_{ii}} = \begin{cases} \mathbf{\Lambda}_{t_{ii}} & \mathbf{\Lambda}_{t_{ii}} \cdot n_t \geq 0; \\ 0 & \mathbf{\Lambda}_{t_{ii}} \cdot n_t < 0. \end{cases} \quad , \quad \mathbf{\Lambda}^-_{t_{ii}} = \begin{cases} \mathbf{\Lambda}_{t_{ii}} & \mathbf{\Lambda}_{t_{ii}} \cdot n_t < 0; \\ 0 & \mathbf{\Lambda}_{t_{ii}} \cdot n_t \geq 0. \end{cases}$$

where n_x, n_y, n_z and n_t define the outward unit normal to an element face for direction x, y, z and t respectively. For orthogonal quadrilateral elements, $n_x = -1$ for faces whose outward normal points anti-parallel to the x-axis, and $n_x = +1$ for faces whose outward normal points parallel to the x-axis, and likwise for the other axes. The Riemann approach allows each axis to be treated as an independent eigenvalue problem. Once formed, the sorting matrices are mapped back in the associative transforms

$$\mathbf{A}^+_x = \mathbf{L}_x \mathbf{\Lambda}^+_x \mathbf{R}_x \tag{5}$$

$$\mathbf{A}^-_x = \mathbf{L}_x \mathbf{\Lambda}^-_x \mathbf{R}_x \tag{6}$$

$$\mathbf{A}^+_y = \mathbf{L}_y \mathbf{\Lambda}^+_y \mathbf{R}_y \tag{7}$$

$$\mathbf{A}^-_y = \mathbf{L}_y \mathbf{\Lambda}^-_y \mathbf{R}_y \tag{8}$$

$$\mathbf{A}^+_z = \mathbf{L}_z \mathbf{\Lambda}^+_z \mathbf{R}_z \tag{9}$$

$$\mathbf{A}^-_z = \mathbf{L}_z \mathbf{\Lambda}^-_z \mathbf{R}_z \tag{10}$$

$\mathbf{A}_x^+$ is placed in the outbound surface integral. This integral is placed on the l.h.s of the matrix equation and is absorbed into the solution. $\mathbf{A}_x^-$ is placed in the inbound surface integral that contains the element boundary conditions. This integral is placed on the r.h.s. of the matrix equation. The matrices $\mathbf{A}_y^+$, $\mathbf{A}_y^-$, $\mathbf{A}_z^+$, $\mathbf{A}_z^-$, $\mathbf{A}_t^+$ and $\mathbf{A}_t^-$ are treated similarly.

4. OPTIMAL LINEAR METHODS

In many demanding transport applications it is necessary to capture sharp gradients in the solution, for example in the vicinity of material boundaries. The discontinuous Galerkin method allows this to some extent by not enforcing continuity of solution at the element boundaries. Although this is adequate for many types of radiation transport problem, there are cases when it produces unwanted oscillation. It is possible to suppress this behaviour by adding on to the discretisation an upwind term for gradient control and numerical stability. This results in a discontinuous Petrov-Galerkin (DPG) formulation that improves robustness of the transport solution while retaining the accuracy. The general form of the angular discretised equation with this modification may be written in conservative form

$$(\mathbf{I} - \nabla \cdot \mathbf{AP})\mathscr{R} = \mathbf{0} \tag{11}$$

in which $\mathbf{P}$ is an angular stabilisation matrix and $\mathscr{R}$ the residual of the governing equation. The choice of $\mathbf{P}$ determines the type of PG scheme. In general, $\mathbf{P}$ is a function of $\mathbf{A}$ and many choices are to be found in the literature. Popular examples are the full Riemann SUPG method and Even Power SUPG method such as that used in the finite element code *RADIANT* [5, 6, 8]. Dissipation is added internal to an element, and the amount that is added can be optimised in various ways to avoid adding in too much diffusion. This is important, as excessive artifical diffusion can heavily reduce accuracy and convergence of the scheme. An example of an optimal method has been published in [7] in which the finite element solution matches the exact solution at each outlet node in one spatial dimension. This is achieved by scaling the amount of dissipation added internal to an element with a parameter α calculated from the cross-section. Similar work was later published in [4] with development of an optimal method for multi-dimensional systems, where an exact solution was not available. This method works by deriving a one-dimensional system along the streamline direction. That is to use $A_s = \mathbf{n}^* \cdot \mathbf{A}$ in which $\mathbf{n}^*$ is defined as a face normal would be defined in a control volume method, i.e. $\mathbf{n}^* = \frac{\nabla \mathbf{N}_i}{|\nabla \mathbf{N}_i|}$ where $\mathbf{N}_i$ is the node i basis function. One may use an appropriate Riemann decomposition of $\mathbf{A}_s$. That is to use $A_s = \mathbf{R}_s \Lambda_s \mathbf{L}_s$ where $\mathbf{R}_s$ and $\mathbf{L}_s$ are the left and right eigenvectors of $\mathbf{A}_s$ and Λ_s the diagonal matrix of eigenvalues associated with the Riemann decomposition of $\mathbf{A}_s$. This allows the derivation of a set of one-dimensional waves. One can then write

$$\Lambda_s \frac{\partial \Psi_s}{\partial s} + \mathbf{H}_s \Psi_s = \mathbf{0} \tag{12}$$

which has analytical solutions, where $\mathbf{H}_s = \mathbf{L}_s \mathbf{H} \mathbf{R}_s$ is the scattering removal operator mapped into the appropriate Riemann space. One-dimensional optimal methods such as those in [7] may then be applied in this space. In [4], a stabilisation matrix $\mathbf{P}$ was defined based on these

one-dimensional considerations in order to remove oscillations from the multi-dimensional solution. In this method, the artificial dissipation is added internal to an element. This choice of $\mathbf{P}$ has the form

$$\mathbf{P} = \mathbf{R}_s \Lambda_s^{-1} \mathbf{G}^T \mathbf{R}_G \Lambda_\alpha \mathbf{L}_G \mathbf{G} \Lambda_s^{-1} \mathbf{L}_s \tag{13}$$

in which $\mathbf{G}^T\mathbf{G} = \mathbf{H}_s$ is the Cholesky factorisation of $\mathbf{H}_s$. One forms the matrix $\mathbf{A}_G = \mathbf{G}^{-T}\mathbf{\Lambda}_s\mathbf{G}^{-1}$, using the Cholesky factors of $\mathbf{H}_s$. This has the eigenvalue decomposition $\mathbf{A}_G = \mathbf{R}_G\mathbf{\Lambda}_G\mathbf{L}_G$, where $\mathbf{R}_G$ and $\mathbf{L}_G$ are the matrices containing the right and left eignevectors respectively, and $\mathbf{\Lambda}_G$ the diagonal matrix of eigenvalues of $\mathbf{A}_G$. The diagonal matrix Λ_α is formed by placing the optimal coefficient α for direction i at position i on the main diagonal. That is to use

$$\mathbf{\Lambda}_{\alpha_{\mu\nu}} = \begin{cases} h|\mathbf{\Lambda}_{G_{\mu\nu}}|\alpha(\hat{\sigma}) & \mu = \nu; \\ \mathbf{0} & \mu \neq \nu. \end{cases}$$

where the optimal coefficient is defined as

$$\alpha = \frac{(6 + 4\hat{\sigma} + \hat{\sigma}^2)e^{-\hat{\sigma}} + 2\hat{\sigma} - 6}{(12 - 6\hat{\sigma}) - (12 + 6\hat{\sigma})e^{-\hat{\sigma}}} \tag{14}$$

Thus the dimensionless cross-section for the set of one-dimensional waves is given by $\hat{\sigma} = \frac{\sigma h}{|\Lambda_G|}$. Inserting the Cholesky factorisation into the angular discretisation ensures that Eq. 12 is diagonal; note that without this approach, the system would not be diagonal in situations where $\mathbf{H}_s$ is not diagonal, for example wavelet methods [17]. The Cholesky factorisation of $\mathbf{H}_s$ makes the resulting stabilisation scheme work for arbitrary angular discretisation. It is found that α assumes a value of 0.25 in voids and tends to this value also in optically thick cases. This is discussed in more detail in section 5.1.

Artificial dissipation in PG methods is characterised by the element length scale which determines the distance across which the dissipation acts. In [7] and [4] the length of the element in space was used. However, this choice becomes inappropriate where there is transient behaviour in which case the element timestep could be a better choice. Where both spatial and temporal gradients are important, neither the spatial length of the element or the timestep are entireley satisfactory. Thus there is ambuguity regarding the type of disspation to use. Section 5 introduces non-linearity into the method of [4] to define a more appropriate type of dissipation.

Non-linearity also allows gradients to be controlled in directions other than that of $\nabla\mathbf{N}_i$.

5. OPTIMAL NON-LINEAR METHODS

Many conventional non-linear SUPG methods use an amount of dissipation that is made optimal in the gradient direction, but acts in the streamline direction [9]. This is achieved by using the angle between the gradient and streamline directions to calculate the projection of the dissipation on the gradient vector. However, where the gradient and streamline are perpendicular the

projection is zero and thus the stabilisation term vanishes. Such approaches are only capable of shock capture where the gradient and streamline are not perpendicular. In the non-linear method presented in the current section, the added dissipation acts in the direction of the solution gradient. This approach allows shock capture even when the gradient and streamline are perpendicular. The dissipation used is made optimal with a method based on that of [4]. In section 4, an optimal stabilisation matrix $\mathbf{P}$ was cited based on the optimal coefficient α in the Riemann space of $\mathbf{A}_s = \mathbf{R}_s\Lambda_s\mathbf{L}_s$. This stabilisation matrix describes the magnitude of numerical dissipation that is introduced to an element to stabilise the solution. The coefficient optimises the magnitude of the dissipation for a particular choice of length scale. In the linear discontinuous Petrov-Galerkin (DPG) method described in section 4, the spatial length of the element is used for this length scale. A disadvantage of this approach is that the same choice of length scale is used everywhere within the solution domain. Use of the element spatial width will become optimal as transient solutions reach steady-state but may be inappropriate at early time while there is time dependent behaviour. Using the element time-step as the length scale will produce optimal dissipation where the temporal gradients dominate over the spatial gradients but becomes inappropriate once steady-state is reached. In general, the direction of the solution gradient $\mathbf{n} \cdot \frac{\nabla\Psi}{|\nabla\Psi|}$ will vary across the problem and may change with time also. Linear methods such as that discussed in section 4 have no knowledge of the solution gradient, and consequently are not guaranteed to be optimal at all points across the domain at all times. Another deficiency they have, also arising from the fact they have no local knowledge of solution gradient, is they are not capable of shock-capture; they introduce dissipation only along the direction of the $\nabla\mathbf{N}_i$ term in the stabilisation. To enable shock-capture, local gradients of the solution must be taken into consideration making the scheme non-linear. The direction in which the dissipation is optimal is then defined locally depending on the solution gradient. In the present section, a method is formulated that is optimal in a direction defined locally depending on the direction of the solution gradient in space-time. Eq. 11 may be generalised to the form

$$(\mathbf{I} - \nabla \cdot \mathbf{A}^*\mathbf{P}^*)\mathscr{R} = \mathbf{0} \tag{15}$$

where $\mathbf{A}^*$ is a modified advection velocity based on the solution gradient $\nabla\Psi \approx \sum_j \nabla\mathbf{N}_j\phi_j$. $\mathbf{A}^*$ will therefore differ in each element due to variations in solution behaviour, and is defined in Eq. 17. $\mathbf{P}^*$ is an $\mathcal{M} \times \mathcal{M}$ angular stabilisation matrix defined according to

$$\mathbf{P}^* = \mathbf{R}_s^*\Lambda_s^{*-1}\mathbf{G}^T\mathbf{R}_G^*\Lambda_\alpha\mathbf{L}_G^*\mathbf{G}\Lambda_s^{*-1}\mathbf{L}_s^* \tag{16}$$

in which $\mathbf{R}_s^*$ and $\mathbf{L}_s^*$ are the matrices containing the right and left eigenvectors of $\mathbf{A}_s^* = \frac{\nabla\mathbf{N}_i}{||\nabla\mathbf{N}_i||} \cdot \mathbf{A}^*$ respectively, and Λ_s^* the diagonal matrix of eigenvalues associated with the Riemann decomposition of $\mathbf{A}_s^*$. Thus $\mathbf{P}^*$ is the same function of $\mathbf{A}^*$ that $\mathbf{P}$ is of $\mathbf{A}$ in Eq. 11. Therefore, the underlying optimal formulation is identical in the NDPG method and the linear method. Eq. 15 may be used as a general form for SUPG equations; note that using $\mathbf{A}^* = \mathbf{A}$ and $\mathbf{P}^* = \mathbf{P}$ results in the standard definition. In the current work, the definition used for $\mathbf{A}^*$ is akin to that used by Donea and co-workers [12]. That is to project the advection velocity $\mathbf{A}$ onto the gradient of the solution. This enables shock capture by ensuring the diffusion acts along the direction of the solution gradient which varies locally rather than acting along the direction of $\nabla\mathbf{N}_i$ at all

solution points in the domain. One projects the advection velocity in this fashion by considering the two vectors $\mathbf{A} = (\mathbf{A}_x, \mathbf{A}_y, \mathbf{A}_z, \mathbf{A}_t)^T$ and $\nabla\Psi = (\frac{\partial\Psi}{\partial x}, \frac{\partial\Psi}{\partial y}, \frac{\partial\Psi}{\partial z}, \frac{\partial\Psi}{\partial t})^T$, and applying the cosine rule. Note that each component of $\nabla\Psi$ is itself a vector of length $\mathcal{M}$, component m of which refers to moment m in the angular expansion of Ψ. Each component of $\mathbf{A}$ is an $\mathcal{M} \times \mathcal{M}$ matrix. The cosine rule defines the angle θ subtended between the vectors $\mathbf{A} = (\mathbf{A}_x, \mathbf{A}_y, \mathbf{A}_z, \mathbf{A}_t)^T$ and $\nabla\Psi = (\frac{\partial\Psi}{\partial x}, \frac{\partial\Psi}{\partial y}, \frac{\partial\Psi}{\partial z}, \frac{\partial\Psi}{\partial t})^T$ as illustrated in Fig. 1. Note that θ is therefore a vector of length $\mathcal{M}$.

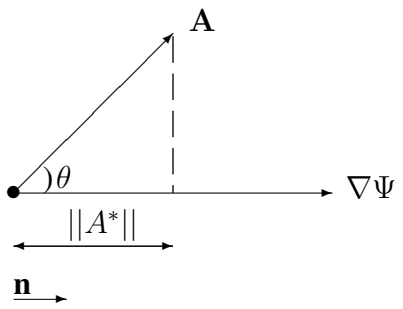

Figure 1. Angle Between Advection Direction and Solution Gradient

The cosine rule states that $\cos\theta = \frac{\mathbf{A}\cdot\nabla\Psi}{||\mathbf{A}||||\nabla\Psi||}$. The direction of the gradient is given by the unit vector $\mathbf{n} = \frac{\nabla\Psi}{||\nabla\Psi||}$. The projection of $\mathbf{A}$ on $\nabla\Psi$ may be written $||\mathbf{A}^*|| = ||\mathbf{A}||\cos\theta$. This is simply the length (or 2-norm) of the vector

$$\mathbf{A}^* = \mathcal{S}\frac{(\mathbf{A}\cdot\nabla\Psi)\nabla\Psi}{||\nabla\Psi||^2} \tag{17}$$

where $||\nabla\Psi|| = \sqrt{(\frac{\partial\Psi}{\partial x}^2 + \frac{\partial\Psi}{\partial y}^2 + \frac{\partial\Psi}{\partial z}^2 + \frac{\partial\Psi}{\partial t}^2)}$ is the Euclidean norm of $\nabla\Psi$. This is simply the geometric length (or 2-norm) of the solution gradient. Thus $||\nabla\Psi||$ is a vector of length $\mathcal{M}$ and $(\mathbf{A}\cdot\nabla\Psi)$ a vector of length $\mathcal{M}$. $\mathcal{S} = -Sign(\mathscr{R})$ is a sign change necessary to ensure the added dissipation is positive, with $Sign(\mathscr{R})$ defined to be a vector of length $\mathcal{M}$ containing either a $+1$ or a -1 in row μ depending on the sign of $\mathscr{R}_\mu$. $\mathbf{A}^*$ is an $\mathcal{M} \times \mathcal{M}$ diagonal matrix defined according to

$$\mathbf{A}^*_{\mu,\nu} = \begin{cases} \mathcal{S}\frac{(\mathbf{A}\cdot\nabla\Psi)_\mu\nabla\Psi_\mu}{||\nabla\Psi||^2_\mu} & \mu = \nu; \\ 0 & \mu \neq \nu. \end{cases}$$

where $\mu = 1, 2, ..., \mathcal{M}$ refers to a particular moment in the angular expansion of Ψ and $(\mathbf{A}\cdot\nabla\Psi)_\mu$ refers to the dot product $(\mathbf{A}\cdot\nabla\Psi_\mu)$. Row μ of the vectors $||\nabla\Psi||^2$ and $\nabla\Psi$ is denoted by $||\nabla\Psi||^2_\mu$ and $\nabla\Psi_\mu$ respectively. It is useful to define also the diagonal matrix $\mathbf{B}$ where

$$\mathbf{B}_{\mu,\nu} = \begin{cases} \mathcal{S}\frac{(\mathbf{A}\cdot\nabla\Psi)_\mu}{||\nabla\Psi||^2_\mu} & \mu = \nu; \\ 0 & \mu \neq \nu. \end{cases}$$

One may then write $\mathbf{A}^* = \mathbf{B}(\mathbf{I}\nabla\Psi)$ where $\mathbf{I}\nabla\Psi$ is used to denote an $\mathcal{M} \times \mathcal{M}$ matrix containing row μ of the vector $\nabla\Psi$ at position μ on the main diagonal.

5.1. Void Treatment

In a material, the optimal NDPG approach discussed relies on a Cholesky factorisation of the scattering removal operator to reliably form a diagonal system of equations in Riemann space. That is to use $\mathbf{H}_s = \mathbf{G}^T\mathbf{G}$ in which $\mathbf{H}_s = \mathbf{L}_s\mathbf{H}\mathbf{R}_s$ is the mapping of the scattering-removal matrix operator into the Riemann space of $\mathbf{A}_s$, and $\mathbf{G}^T$ and $\mathbf{G}$ are the Cholesky factors of $\mathbf{H}_s$. These Cholesky factors are defined only if $\mathbf{H}_s$ has a positive non-zero eigenstructure. The strength of this approach is that it allows the optimal scheme to be applied within any angular discretisation framework, as a diagonal system can easily be formed. In a void, the problem reduces to pure advection comprising only the streaming term. The $\mathbf{H}$ term is absent from the equation and so the $\mathbf{H}_s$ Riemann term is not present in the one-dimensional diagonal equation. Consequently, the system along the streamline in a void is simply

$$\mathbf{\Lambda}_s\frac{\partial\Psi_s}{\partial s} + \alpha h\mathbf{\Lambda}_s\frac{\partial}{\partial s}(\mathbf{\Lambda}_s\frac{\partial\Psi_s}{\partial s}) = \mathbf{0} \tag{18}$$

where h is the length scale, typically $h = \frac{\Delta x}{4}$ or $h = \frac{\Delta x}{2}$ and Δx is the width of the element. α is the optimal coefficient for the artificial dissipation in a void. By examining the DG stencil of Eq. 18 using this choice of length scale, one finds that $\alpha = 0.25$ matches the analytical solution at the outlet node of the element. Selecting this choice of α in elements that contain a void, while using the previous definition elsewhere, one has an NDPG scheme that can stabilise transport solutions across all regimes. It is shown in [4] that α approaches 0.25 in the optically thick case also. It is left as the topic of future work to assess how good an approximation it is to use $\alpha = 0.25$ throughout the domain, which would preclude the need for the Cholesky factorisation in Eq. 16. There is strong motivation to attempt this, as it would improve on the efficiency of the NDPG method.

5.2. Length Scale

It is necessary to multiply the upwind term by a characteristic length h. This determines the distance into the element the acting diffusion is to be applied. Conventional Petrov-Galerkin formulations often use $h = \frac{\Delta x}{2}$ as this characteristic length, in which Δx is the width of the finite element in space. This correctly centres the equation residual at the centre of mass (CoM) of the basis function, for continuous finite element representations. In the present work, where discontinuous finite elements are used to formulate the space-time discretisation, the CoM of the basis function is centred a distance $\frac{\Delta x}{4}$ from the upwind boundary of the element. It is recommended therefore, that $h = \frac{\Delta x}{4}$ be used with the NDPG method instead of $h = \frac{\Delta x}{2}$. This translates the equation residual along the gradient of the basis function adding additional

upwinding to the NDPG finite element stencil, correctly positioning the residual calculation at the CoM of the discretisation. This is important for ensuring the method uses the correct amount of upwinding. The finite element stencil for the standard DG method without using any added dissipation is shown to be

$$\begin{bmatrix} -1 & \frac{1}{2} & \frac{1}{2} & 0 & 0 \\ 0 & -\frac{1}{2} & \frac{1}{2} & 0 & 0 \end{bmatrix}$$

while the NDPG stencil, using $h = \frac{\Delta x}{4}$, is found to be

$$\begin{bmatrix} -1 & \frac{3}{4} & \frac{1}{4} & 0 & 0 \\ 0 & -\frac{3}{4} & \frac{3}{4} & 0 & 0 \end{bmatrix}$$

Examining these two stencils, one can see that using $h = \frac{\Delta x}{4}$ for the characteristic length in the NDPG discretisation amounts to increasing the upwinding by 50%, with respect to standard DG. Interestingly, the downwind balance remains unaltered. Note this is akin to shifting the residual calculation upwind along the gradient by using $(x_0 - \frac{\Delta x}{4})$ in the Taylor expansion of $\mathscr{R}$, about the origin x_0 of the discontinuous finite element. Note that the stencil for standard PG methods using $h = \frac{\Delta x}{2}$ is

$$\begin{bmatrix} -1 & 1 & 0 & 0 & 0 \\ 0 & -1 & 1 & 0 & 0 \end{bmatrix}$$

6. NUMERICAL EXAMPLES AND DISCUSSION

In this section results are presented for the NDPG optimal solver algorithm using different angular schemes. These include the spherical harmonics method and the discrete ordinates method. The non-linear scheme is demonstrated for a set of demanding radiation transport problems that include time dependent and steady-state cases.

6.1. Problem 1: Time Dependent Absorber

Fig. 2 illustrates in the solution domain of problem 1, the time dependent absorber. This calculation is performed on a three dimensional Cartesian (x,y,z) mesh, with the spatial domain in the x,y plane and the time domain along the z-axis. A $12\times12\times12$ element mesh is used for this configuration. Material properties used are shown in Tab. I. A cross-section of 7cm^{-1} is used throughout the spatial part of the domain. An imposed radiation source is located in the range 5cm $\leq$ x $\leq$ 8cm, 5 cm $\leq$ y $\leq$ 8 cm. The cross-section is significant, and combined with the relatively low spatial and temporal resolution makes this a very demanding problem for the standard DG method. The original linear optimal method, shown to work well for steady-state solutions, is shown to perform quite poorly for this problem in Fig. 3. This plot comprises line-outs of the scalar flux solution through the centre of the mesh and parallel to the x,y axes (Line-Out A) and through time parallel to the temporal axis (Line-Out B). The DG solution shows

severe oscillation due to the inadequate spatial and temporal resolution. The linear optimal method degrades the solution to this problem considerably, introducing large oscillations in the time direction that are not seen on the standard DG solution. Introducing non-linearity totally removes these oscillations, and the new non-linear NDPG scheme stabilises the transport solution very effectively. This is demonstrated in Fig. 4 for (a,b) a P_3 approximation and (c,d) an S_4 approximation. The NDPG scheme perfoms consistently well for both angular approximations, fully stabilising the finite element solution. The exact solution is plotted for benchmarking. This shows that the NDPG method improves accuracy as well as robustness.

6.2. Problem 2: Void

The NDPG method offers an effective remedy for oscillation in voids, where other schemes may perform poorly. To demonstrate the void treatment using the NDPG scheme, the two dimensional domain illustrated in Fig. 5 was used. This comprised a 12 cm $\times$ 12 cm region driven along the left and lower boundaries with a flux of 1.0 ncm^{-2}s^{-1}, using pure advection to produce a ray at $45\mathrm{deg}$ across the mesh. Scalar flux line-outs across the centre (Line-Out A) and along the top edge (Line-Out B) of the domain are presented for each method on coarse and fine spatial grids in Fig. 6. For these calculations, an S_2 angular approximation was used, in order to produce a well defined ray. The sharp front of the ray is clearly visible on both grids for both methods, and places strain on the spatial approximation causing additional oscillation when stabilisation is not used. These oscillations are smoothed extremely effectively by the NDPG method using just 20 non-linear matrix iterations, along both line-outs. Note that even on a fine mesh, the DG result exhibits significant oscillation. The NDPG method, however, is free from this oscillation that arises from inadequacies of the DG spatial differencing scheme.

6.3. Problem 3: Heavy Absorber Problem

The third test case is illustrated in Fig. 7. The material properties are shown in Tab. II. This problem is difficult to stabilise because oscillations occur in the direction of the solution gradient. It is therefore an important test for the NDPG method. The problem comprises a source region in the range 1cm $\leq$ x $\leq$ 2cm, 1 cm $\leq$ y $\leq$ 2 cm. This is located inside a heavy absorber in the range 0cm $\leq$ x $\leq$ 2cm, 1 cm $\leq$ y $\leq$ 2 cm. Results for the DG and NDPG schemes are illustrated in Fig. 8. Four line-outs are shown. Line-out A in Fig. 8a is through the centre of the domain in the x direction, with line-out B in Fig. 8b showing details at the corner of the peak. Line-out C in Fig. 8c is through the centre of the domain in the y direction, with details at the corner of the peak shown in Fig. 8d for this direction. The DG scheme produces oscillations all the way round the edge of the source peak. These are clearly visible in the line-outs. The NDPG removes these oscillations from the transport solution very effectively in this problem. This is achieved by applying the dissipation only in the gradient direction.

6.4. Convergence

An attempt has been made to improve the convergence rate of the NDPG matrix iteration. Improvement is achieved by slowing down the rate of convergence by combining the solution Ψ_k from the current iteration k with the old solution Ψ_{k-1} from the previous iteration k-1. Each of these two solutions is weighted with a relaxation parameter $0.0 \leq \omega \leq 1.0$. The matrix solve is

then advanced using the variable $\Psi_{k+1} = \omega\Psi_k + (1-\omega)\Psi_{k-1}$. Fig. 9 shows the effect that different relaxation parameters ω have on the NDPG matrix solve, where the 2-norm is plotted against iteration number. Convergence is approached more smoothly with a greater amount of relax, although many more iterations result. Reducing the amount of relax heavily reduces the required number of iterations to achieve a given error however the approach is less smooth. For the simulations presented in this report, a relaxation parameter $\omega = 0.5$ is used. It is sometimes beneficial to use an adaptive relax. This is implemented by reducing the value of ω in response to a change in the behaviour of the convergence during the iteration process. For example, the value of ω could be reduced by a factor 2 each time the behaviour of the 2-norm of the solution changes between non-linear matrix iterations. Another alternative is to optimise the relaxation parameter, by solving $\Psi_{k+1} = \omega\Psi_k + (1-\omega)\Psi_{k-1}$ for the value of ω that minimises the 2-norm of the system. Such a topic is left for the subject of future work.

7. CONCLUSIONS

A new non-linear discontinuous Petrov-Galerkin (NDPG) method is presented that is extremely effective for removing oscillations in the solution to the Boltzmann Transport Equation in transient and steady-state radiation transport applications. The method applies artificial dissipation internal to an element via a novel finite element Riemann approach, in the direction of the solution gradient. Conventional linear stabilisation methods such as SUPG apply dissipation in the direction of the streamline rather than the direction of the solution gradient. Such methods use the same length scale throughout the solution domain, and tend not to remove oscillation from the solution gradient direction. There are a class of problems that exhibit additional oscillation in the gradient direction that therefore cannot be stabilised by conventional streamline upwind methods. By using a gradient-informed scaling of the advection velocity, the new method is able to smooth this type of oscillation extremely effectively in a variety of radiation transport problems. Results have been presented for a set of demanding steady-state and time dependent test problems. Methods for improving the convergence rate of the non-linear iteration used in the NDPG method have been presented. This includes an adaptive relaxation method that dramatically reduces the number of iterations needed to achieve highly converged solutions to the problem.

ACKNOWLEDGEMENTS

The author wishes to acknowledge the Computational Physics Group at AWE for their support during the undertaking of this work. The method presented herein has been developed as part of a PhD project in a collaborative effort between Imperial College London and AWE. Sponsorship of this PhD has been provided by AWE plc. The support of the Applied Modelling and Computation Group at Imperial College London is greatly appreciated.

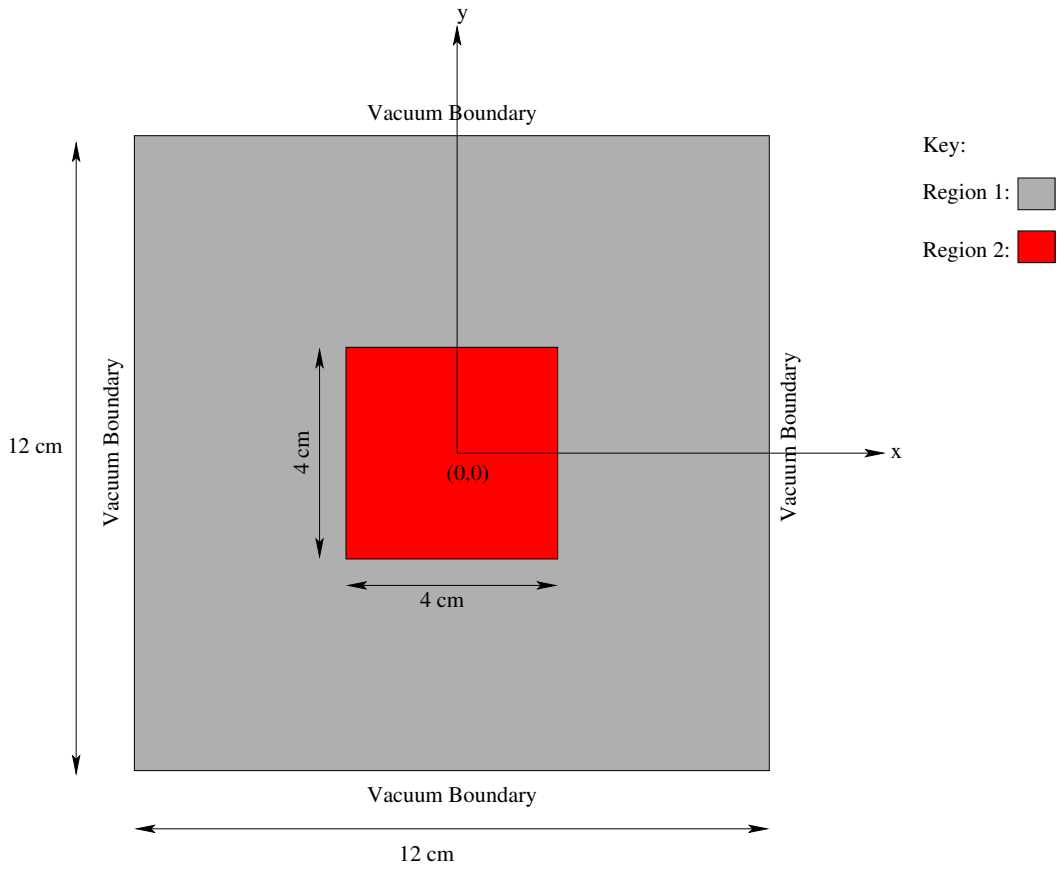

Figure 2. The Time Dependent Absorber Problem

Table I. Time Dependent Absorber Properties

Material Region	Source (n s^{-1})	σ_t (cm^{-1})	σ_s (cm^{-1})
1	0.0	7.0	0.0
2	1.0	7.0	0.0

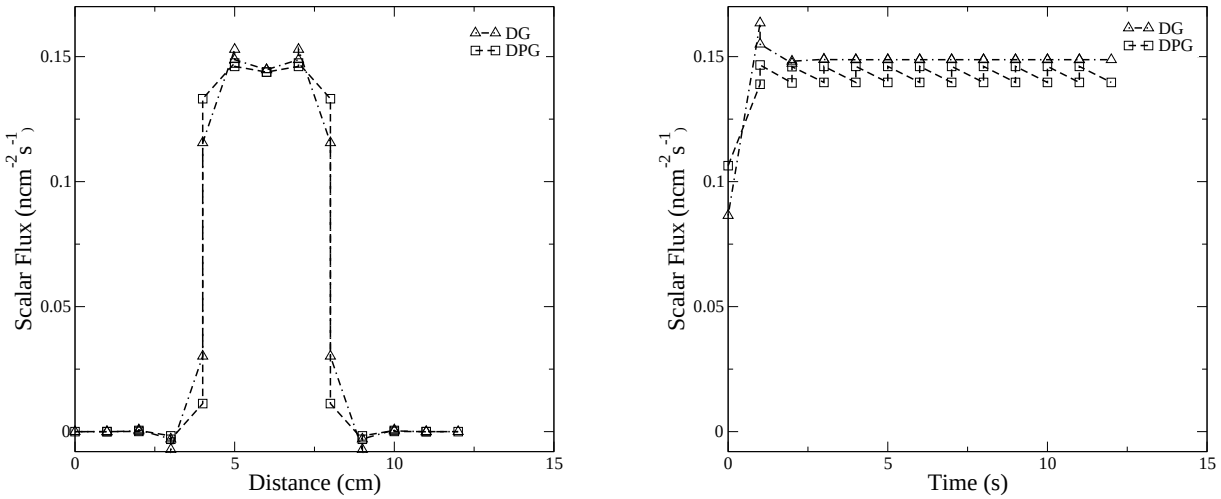

(a) Line-Out A (b) Line-Out B

Figure 3. DG and DPG Scalar Flux Solutions to the Time Dependent Absorber

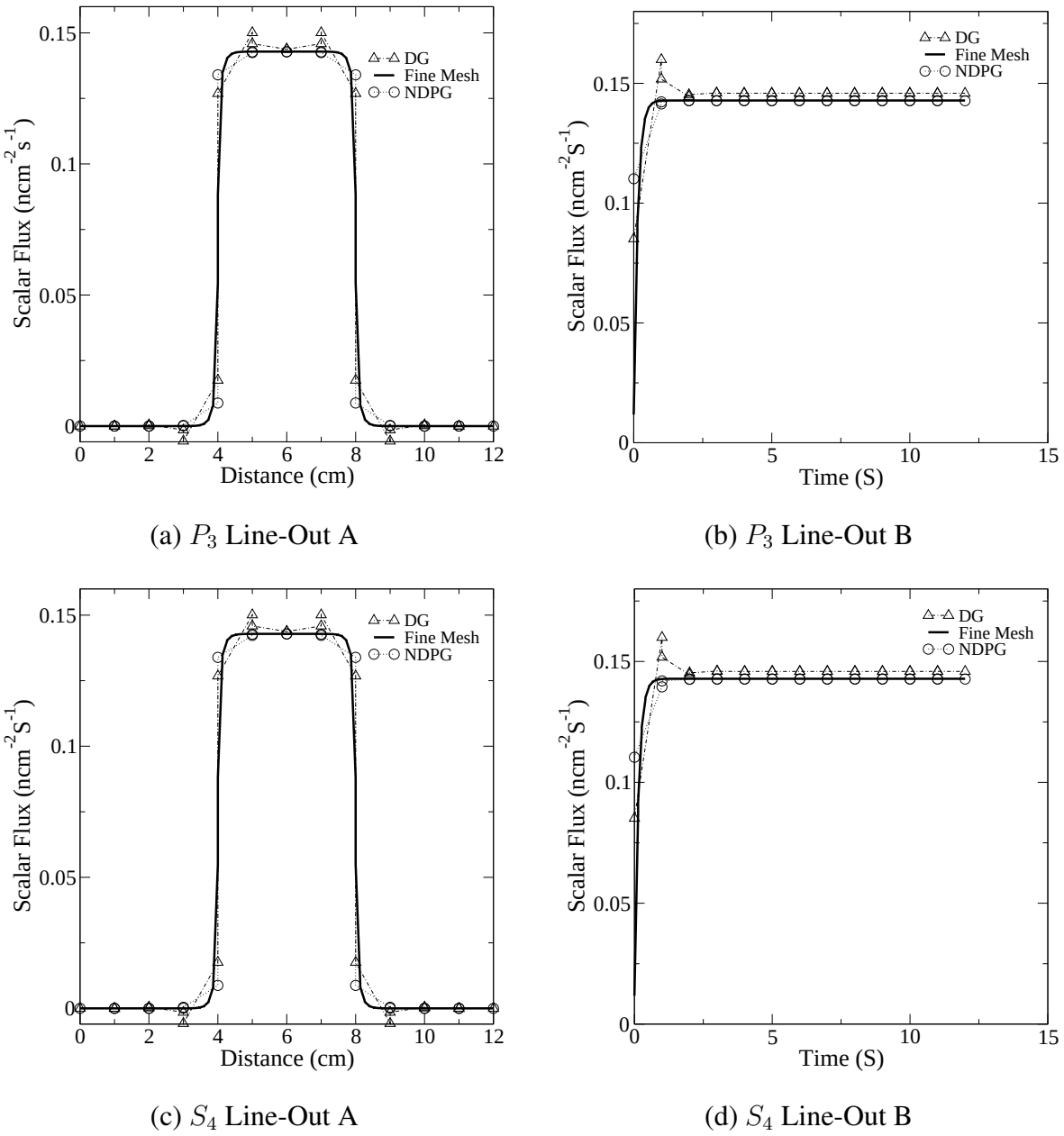

(a) P_3 Line-Out A

(b) P_3 Line-Out B

(c) S_4 Line-Out A

(d) S_4 Line-Out B

Figure 4. DG and NDPG Scalar Flux Solutions to the Time Dependent Absorber

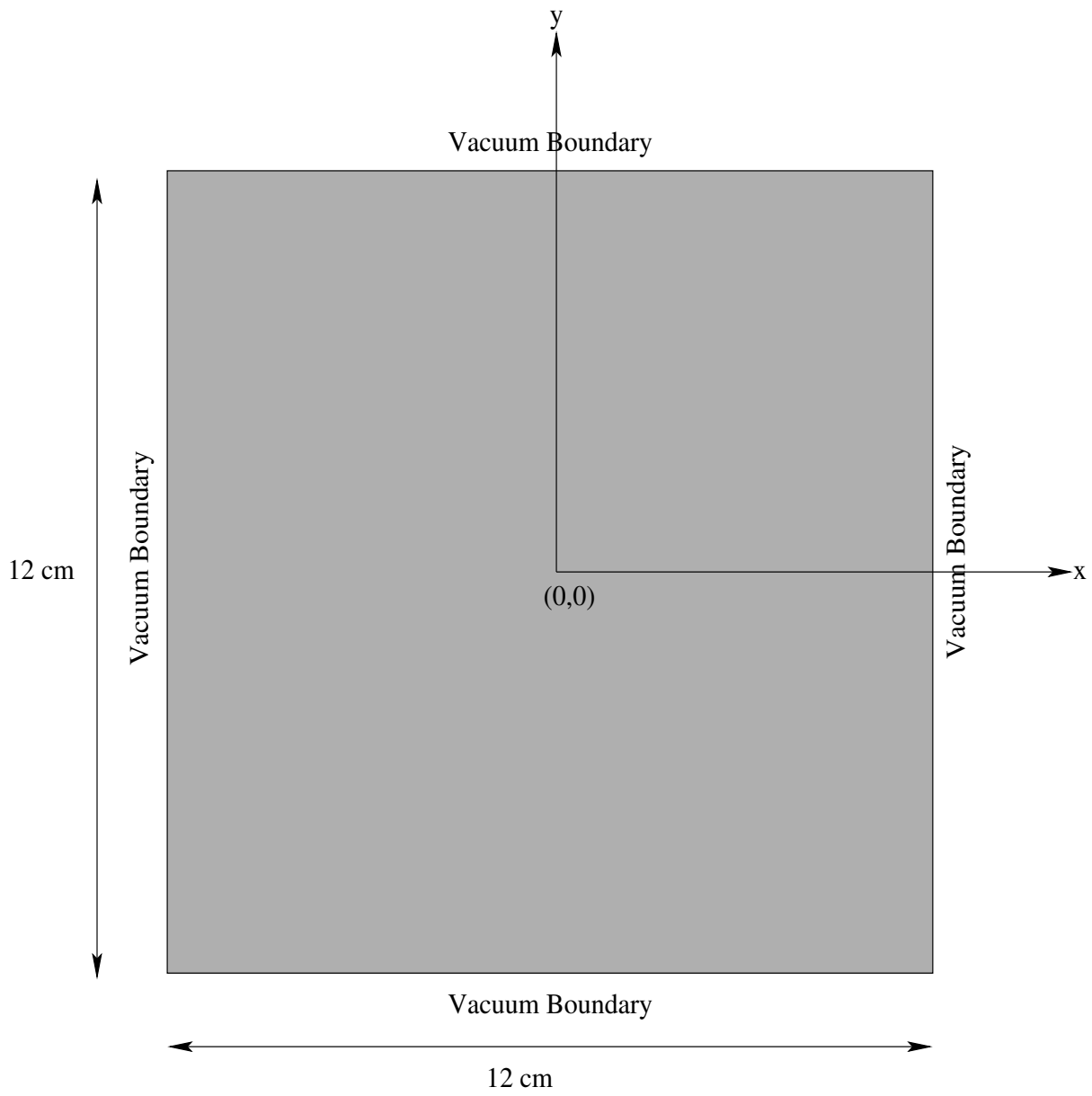

Figure 5. The Void Problem

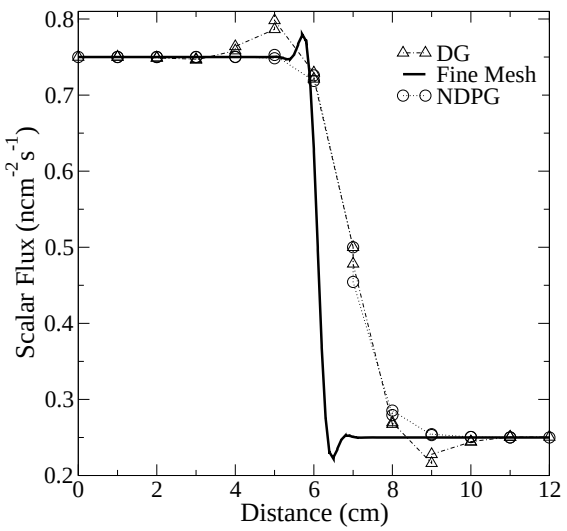

(a) Coarse Mesh Line-Out A

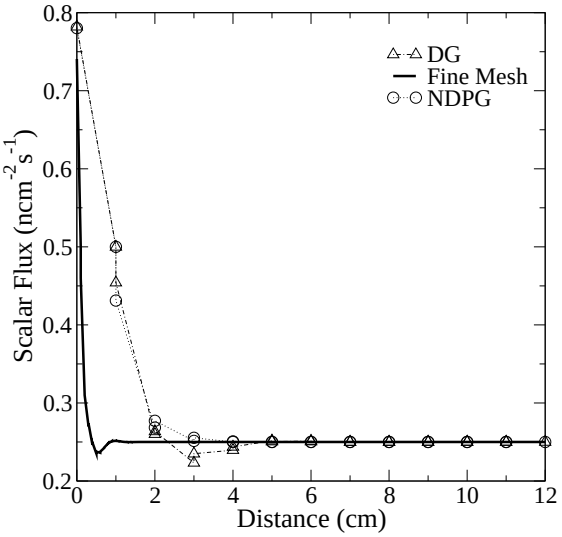

(b) Coarse Mesh Line-Out B

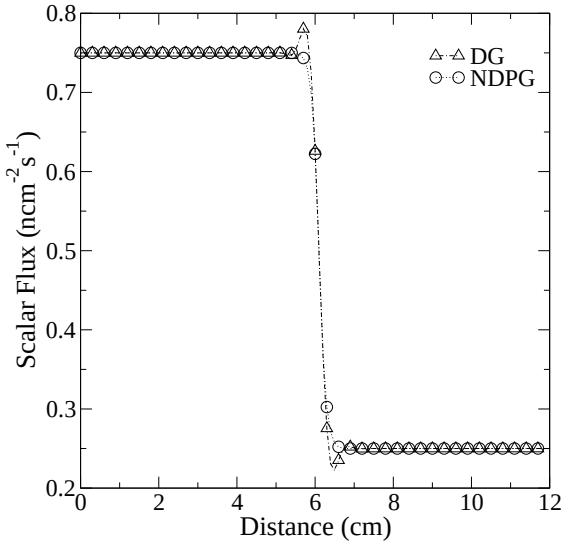

(c) Fine Mesh Line-Out A

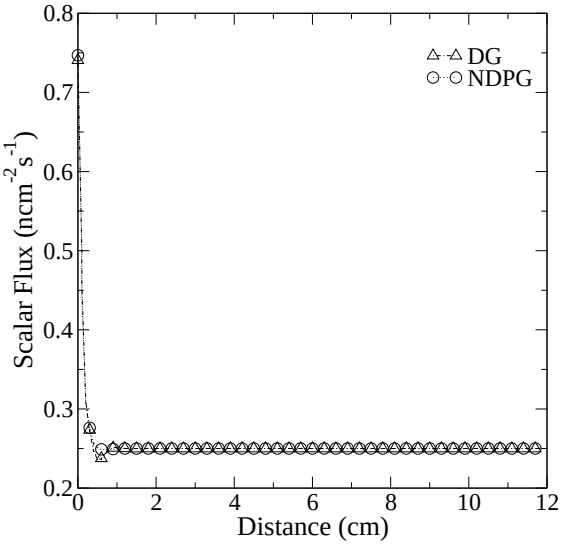

(d) Fine Mesh Line-Out B

Figure 6. Scalar Flux Line-Outs Through the Void Problem

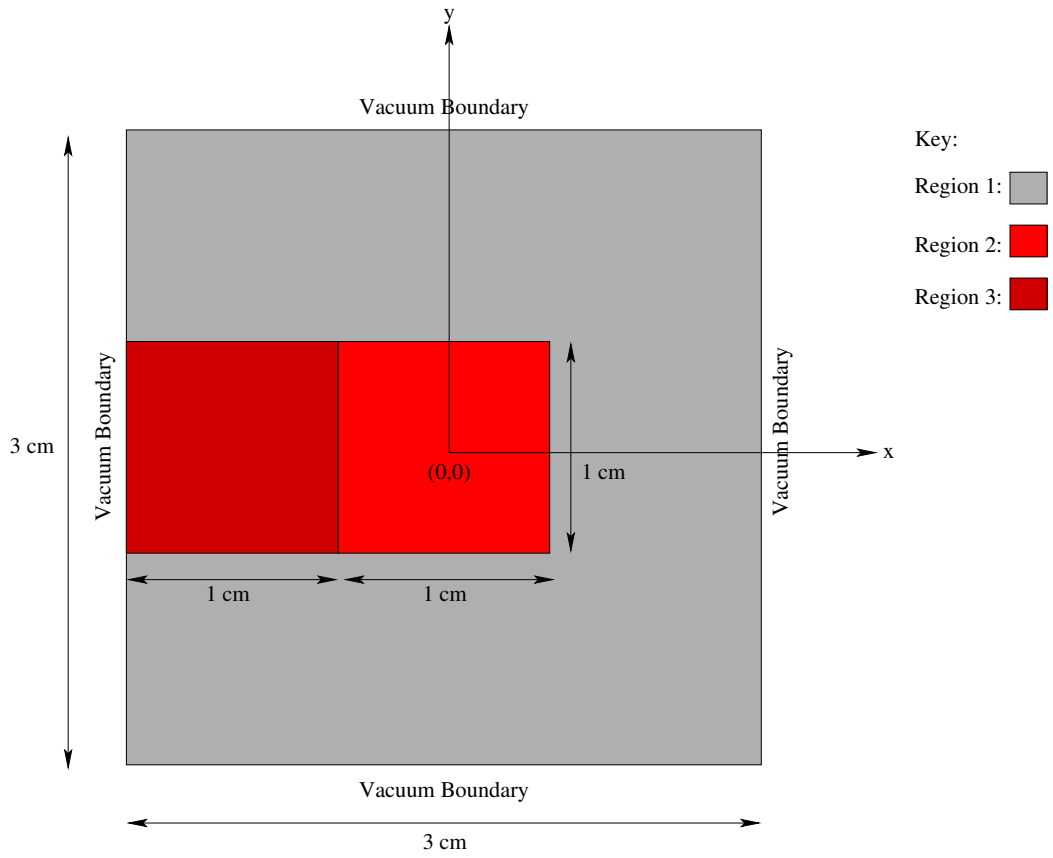

Figure 7. The Heavy Absorber Problem

Table II. Heavy Absorber Properties

Material Region	Source (n s^{-1})	σ_t (cm^{-1})	σ_s (cm^{-1})
1	0.0	0.1	0.0
2	0.0	1000.0	0.0
3	1.0	1000.0	0.0

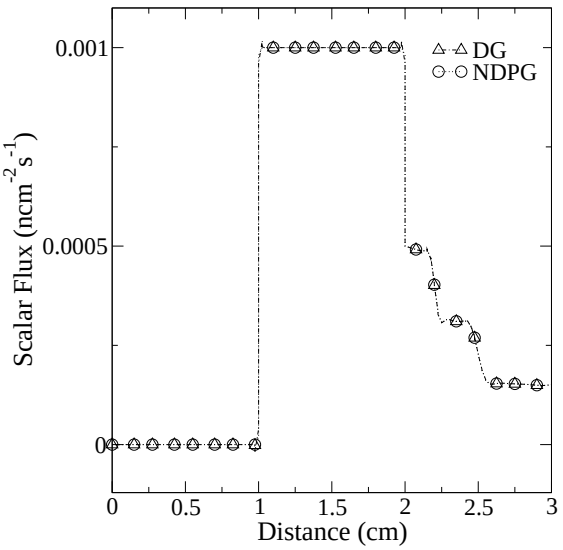

(a) Line-Out A

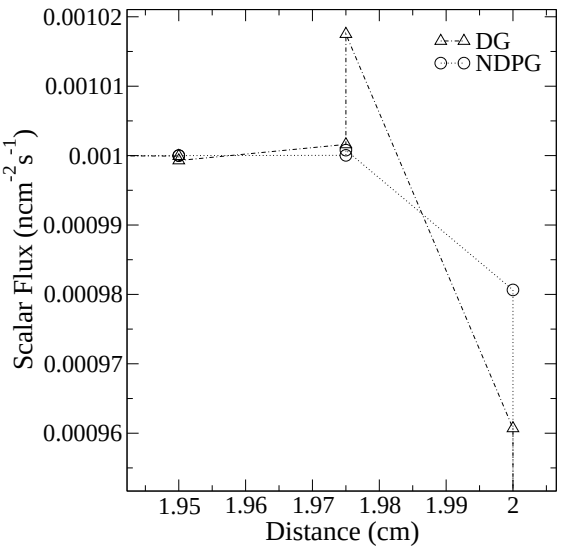

(b) Line-Out B

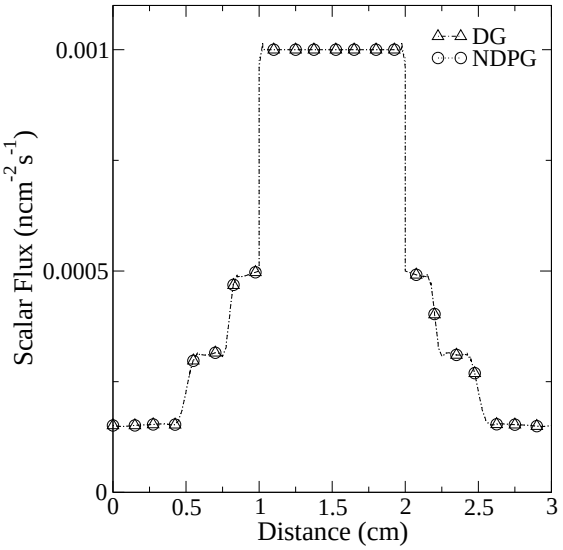

(c) Line-Out C

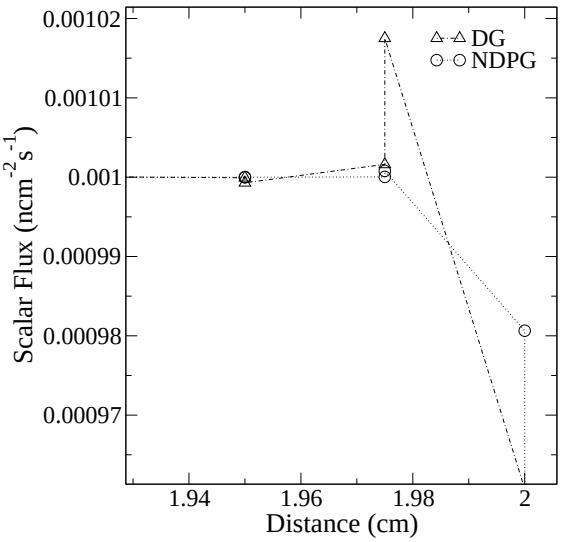

(d) Line-Out D

Figure 8. Scalar Flux Line-Outs Through the Heavy Absorber

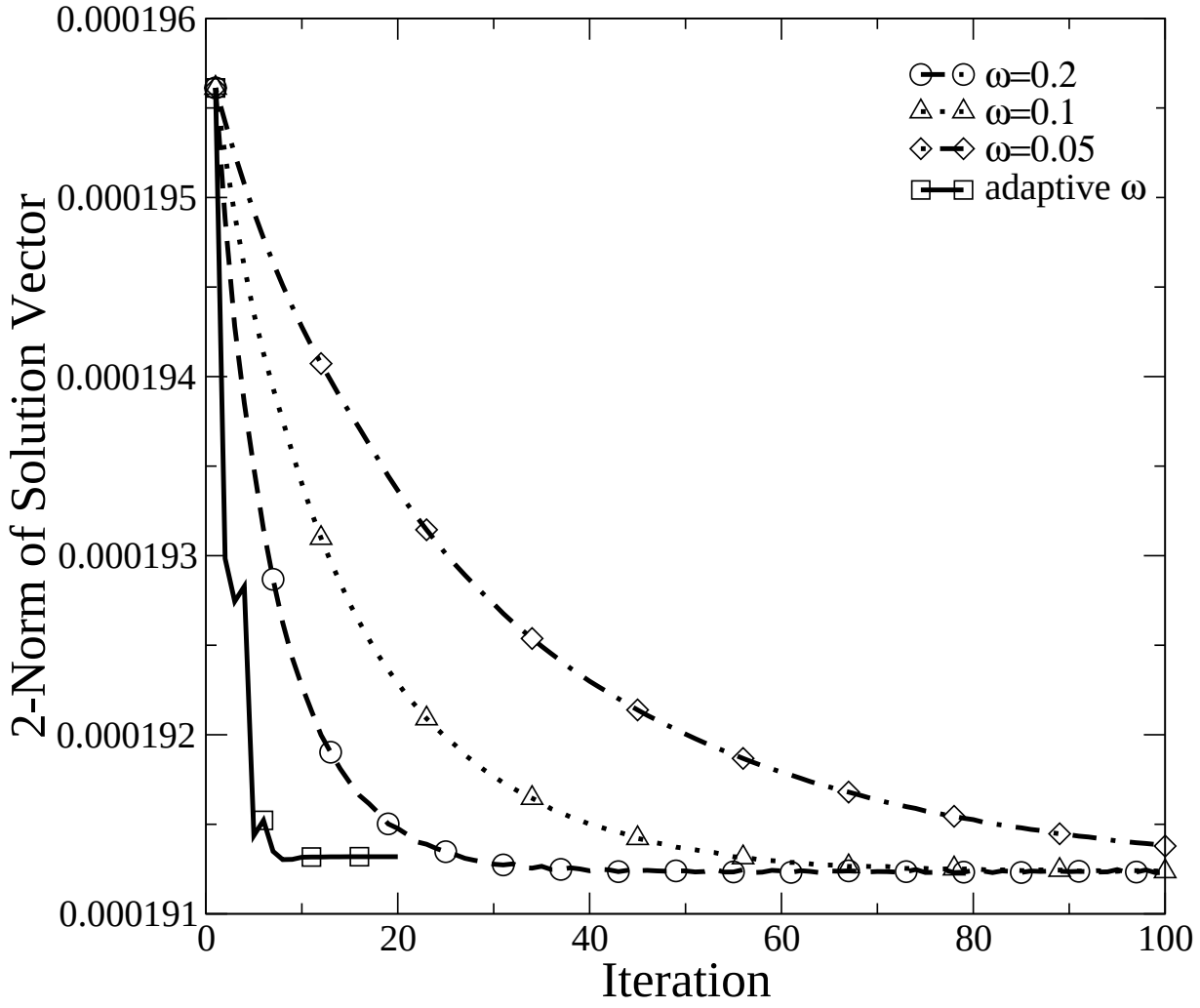

Figure 9. Effect of Different Relaxation Parameters on Convergence of the NDPG Matrix Iteration

REFERENCES

[1] W. H. Reed and T. R. Hill, "Triangular Mesh Methods for the Neutron Transport Equation," Los Alamos Technical Report, **LA-UR-73-479**, (1973).

[2] A. N. Brooks and T. J. R. Hughes, "Streamline Upwind/Petrov-Galerkin Formulations for Convection Dominated Flows with Particular Emphasis on the Incompressible Navier-Stokes Equations," *Computational Methods in Applied Mechanics and Engineering*, **32**, pp. 199-259 (1982).

[3] Yingda Cheng and Chi-Wang Shu, "A Discontinuous Galerkin Finite Element Method For Time Dependent Partial Differential Equations With Higher Order Derivatives," *Mathematics of Computation*, **S 0025-5718(07)02045-5**, (2007).

[4] S. R. Merton, C. C. Pain, R. P. Smedley-Stevenson, A. G. Buchan and M. D. Eaton, "Optimal Discontinuous Finite Element Methods for the Boltzmann Transport Equation

with Arbitrary Discretisation in Angle," *Annals of Nuclear Energy*, **35**, pp. 1741-1759 (2008).

[5] C. C. Pain, M. D. Eaton, R. P. Smedley-Stevenson, A. J. H. Goddard, M. D. Piggott and C. R. E. de Oliveira, "Space-Time Streamline Upwind Petrov-Galerkin Methods for the Boltzmann Transport Equation," *Computer Methods in Applied Mechanics and Engineering*, **195**, pp. 4334-4357 (2006).

[6] C. C. Pain, M. D. Eaton and R. P. Smedley-Stevenson, "Streamline Upwind Petrov-Galerkin Methods for the Steady-State Boltzmann Transport Equation," *Computer Methods in Applied Mechanics and Engineering*, **195**, pp. 4448-4472 (2006).

[7] C. C. Pain and A. J. H. Goddard, "Dual Basis and Characteristic Discontinuous Finite Element Discrtetizations for the Boltzmann Transport Equation," *Transport Theory and Statistical Physics*, **29(6)**, pp. 681-697 (2000).

[8] S. J. Sherwin and R. M. Kirby, "Streamline Upwind Petrov-Galerkin Methods for the Boltzmann Transport Equation," *International Journal for Numerical Methods in Engineering*, **65**, pp. 752-784 (2006).

[9] M. D. Eaton, "A High-Resolution Riemann Method for Solving Radiation Transport Problems on Unstructured Meshes," PhD Thesis, Imperial College London, (2004).

[10] J. K. Fletcher, "A Solution of the Neutron Transport Equation using Spherical Harmonics," *Journal of Physics A: Mathematical and General*, **16**, pp. 2827-2835 (1983).

[11] C. Yildiz, "P_N Solutions of the Time-Dependent Neutron Transport Equation with Anisotropic Scattering in a Homogeneous Sphere," *Journal of Physics D: Applied Physics*, **33**, pp. 704-710 (2000).

[12] J. Donea and A. Huerta, *Finite Element Methods for Flow Problems*, WileyBlackwell, New York & USA (2003).

[13] T. J. R. Hughes and T. E. Tezduyar, "Finite Element Methods for First-Order Hyperbolic Systems with Particular Emphasis on the Compressible Euler Equations," *Computer Methods in Applied Mechanics and Engineering*, **45**, pp. 217-284 (1984).

[14] T. J. R. Hughes and M. Mallet and A. Mizukami, "A New Finite Element Formulation for Computational Fluid Dynamics: II. Beyond SUPG," *Computer Methods in Applied Mechanics and Engineering*, **54**, pp. 341-355 (1986).

[15] T. J. R. Hughes and M. Mallet and A. Mizukami, "A New Finite Element Formulation for Computational Fluid Dynamics: III. The Generalised Streamline Operator for Multidimensional Advective-Diffusive Systems," *Computer Methods in Applied Mechanics and Engineering*, **58**, pp. 305-328 (1985).

[16] T. J. R. Hughes and L. P. Franca and M. Mallet, "A New Finite Element Formulation for Computational Fluid Dynamics: VI. Convergence Analysis of the Generalised SUPG Formulation for Linear Time-Dependent Multidimensional Advective-Diffusive Systems," *Computer Methods in Apllied Mechanics and Engineering*, **63**, pp. 97-112 (1987).

[17] A. G. Buchan et al, "Linear and Quadratic Octahedral Wavelets on the Sphere for Angular Discrtetisations of the Boltzmann Transport Equation," *Annals of Nuclear Energy*, **32**, pp. 1224-1273 (2005).